Original research

Using geostatistics and GIS approaches to characterize and map soil spatial variability in the Nubian Nasr Area of Aswan Governorate, Egypt

Mohamed A.A. Shaalan*, Ahmed Ghallab, Ahmed A.M. Awad, Alaa H. Abd-Elazem

Soil and Natural Resources Department, Faculty of Agriculture and Natural Resources, Aswan University, Aswan 81528, Egypt.

© *Unit of Environmental Studies and Development, Aswan University*

Abstract:

Precision agriculture heavily relies on detailed spatial information about soil characteristics to promote long-term soil and plant health. The present research sought to evaluate, predict, map, and analyze the spatial variability of physicochemical properties in the Nubian Nasr Area of Aswan Governorate. Soil properties were measured, including electrical conductivity, texture, organic matter, calcium carbonate, pH, cation exchange capacity, exchangeable sodium percentage, available nutrients, and sodium absorption ratio. The mean values of the studied soil properties ranged from 2.85 to 449.58, with high values observed for available potassium, sand, available nitrogen, and CEC, and low values for other properties. The geographical distribution of these attributes was mapped and characterized using classical and geostatistical approaches. Spatial variability was quantified using semi-variogram models, and maps of projected values were created using ordinary kriging. Results indicated significant spatial variability in soil properties, with strong correlations between certain parameters. The semi-variogram models that were determined to be best appropriate for the qualities under study were the exponential, Gaussian, K-Bessel, and J-Bessel models. The maps produced offer vital data for precision farming, allowing customized management plans to enhance soil health. Geostatistical techniques effectively characterized, predicted, and mapped spatial soil variability.

Key words: Soil properties, Spatial variability, Geostatistic, Ordinary Kriging, Semi-variogram models.

1. Introduction

Several factors, such as land use, topography, parent material, organisms, human intervention, and time, significantly influence the spatial variation of soil properties (**John et al., 2021; Rosemary et al., 2017**). A deeper understanding of the vertical distribution of soil characteristics across different soil layers can enhance land management practices (**Bogunovic et al., 2017**).

_____

Corresponding author*: E-mail address: mohamed.abdelrahim@agr.aswu.edu.eg

The interaction of biological, natural, and chemical processes leads to considerable soil variability **(Ghartey et al., 2012; Serrano et al., 2014)**. To better understand the complex relationships between soil properties and environmental factors, it is essential to map the spatial distribution of these properties. This knowledge is critical for assessing agricultural potential. By gaining insight into the spatial distribution of soil characteristics, we can optimize agricultural management strategies, tailor inputs to specific field conditions, and make informed decisions **(Fathi et al., 2014)**. The identification and potential implementation of soil heterogeneity by data modeling is very important to increase land use efficiency, agricultural productivity, and ecological sustainability **(Timuçin Everest and Gür, 2022; Ouallali et al., 2024)**. Monitoring and mapping these variations can significantly improve nutrient management practices, leading to increased agricultural productivity and enhanced food security **(Shalaby et al., 2017; Brevik et al., 2016; Lima et al., 2019)**.

Soil mapping and analysis are significantly improved with GIS tools. These tools offer a rapid, cost-effective, precise, and environmentally friendly alternative to traditional methods. Furthermore, geostatistical techniques within GIS provide the ability to accurately estimate soil properties in unmeasured locations and understand how various factors impact soil patterns (Webster and Oliver, 2007). To optimize agricultural practices and meet the specific needs of various soil and crop types, understanding the spatial variation of soil properties is essential **(Jabro et al., 2010; Fraisse et al., 1999; Cruz et al., 2011)**. This knowledge is also crucial for maximizing soil sampling techniques **(Goenster-Jordan et al., 2018)**. Geostatistical methods are effective tools for analyzing the locative patterns and variability of characteristics of soil **(AbdelRahman et al., 2021; John et al., 2021; Liu et al., 2014; Zhang et al., 2015)**. By leveraging spatial relationships between sampled and unsampled locations, these techniques can accurately predict soil parameters, reducing uncertainty and costs **(AbdelRahman et al., 2021).**

GIS technology facilitates the efficient processing of large amounts of spatial data, offering more precise insights into soil properties. Comprehending the temporal and spatial variations in soil characteristics is essential for assessing the impact of agricultural practices on the environment **(Arnous and Hassan, 2006; Goenster-Jordan et al., 2018)**. Kriging, a powerful geostatistical interpolation technique, is widely used in various agricultural applications. Researchers have applied GIS and geostatistical methods to spatially interpolate soil properties, evaluate land, and assess land suitability **(Nada et al., 2022; Abdullahi et al., 2023; Okashaa, 2023)**. The choice of kriging model count on the properties of the data and the desired spatial model. Ordinary kriging (OK) is widely applied for predicting the spatial distribution of soil parameters **(Tang et al., 2017; John et al., 2021)**. However, OK does not consider the potential influence of other environmental factors on the spatial patterns of soil properties **(Ferreiro et al., 2016; AbdelRahman et al., 2021)**.

The Nubian Nasr region, situated in the Nile Valley's eastern region, is part of the Eastern Desert. This area, an extension of the Kom Ombo basin to the east of Aswan, is likely to share the same

geological origins. The region's topography is mostly flat, covered by sand and gravel deposits from an ancient east-west river channel that predates the current Nile River **(Issawi et al., 2016)**. The main objectives of this study were: (1) to assess the significant soil physicochemical properties of the investigation region using geostatistical analysis, and (2) to use GIS and geostatistical techniques to map the spatial variation of these soil properties. The objective is to provide a decision-making framework and guide future planning for the studied area.

2. Materials and Methods

2.1. Area of study

The area under study is part of the Eastern Egyptian Desert in Aswan Governorate; it is situated between latitudes 24° 27' 30" and 24° 35' 0" N and longitudes 33° 0' 0" and 33° 6' 0" E (Fig. 1) and covers an area of 107.51 Km^2 (10750.64 hectares). The study region, located in the Eastern Desert along the Nile Valley, is geologically linked to the Kom Ombo basin. Its flat landscape is characterized by ancient sand and gravel deposits, remnants of a river system older than the present-day Nile **(Issawi et al., 2016)**.
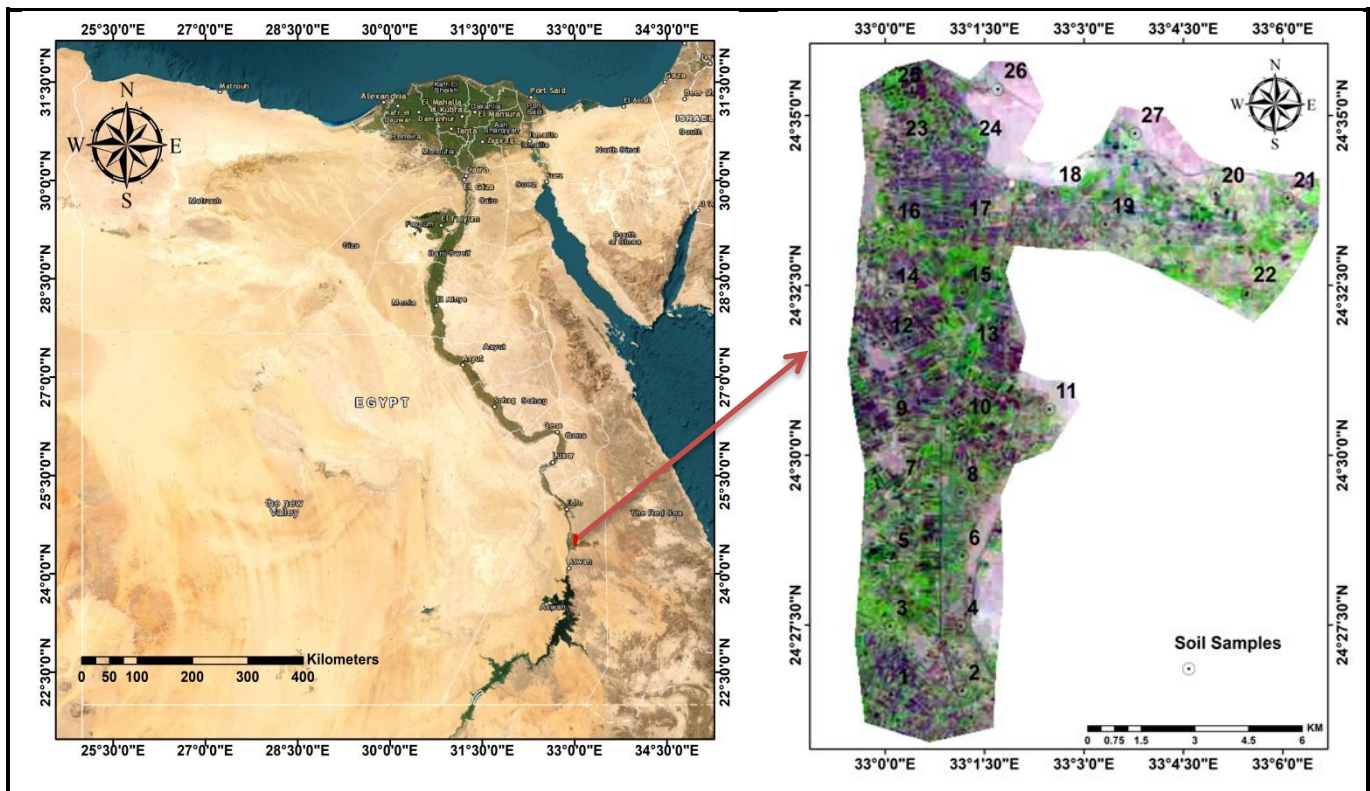

Figure 1: A map showing the study area location

2.2. Soil sampling and laboratory analysis

To represent each type of land and different geographical features, eighty-one soil samples were collected from 27 soil profiles. Soil profiles have from a depth of 120 to 150 cm. Soil samples were Air-dried, crushed, and sieved through a 2-mm sieve in preparation for physical and

chemical testing. An EUTECH conductivity meter was used to test the electrical conductivity (EC), and a HANNA pH meter was used to assess the pH of the generated 1:1 soil-water combination. The percentages of clay were calculated using the pipette method, silt, and sand fractions **(Richards, 1954)**; a calcimeter was used to calculate the lime contents **(Soil Survey, 1992)** and the Walkley-Black method, modified by Jackson **(Jackson, 1958)**, was used to calculate the organic matter. Capacity for cation exchange (CEC) was computed using the sodium acetate-ammonium acetate technique (Richards, 1954). Available Nitrogen (N) was determined using the Kjeldahl method **(Subbiah and Asija, 1956)**. Available phosphorus (P) was measured calorimetrically using a Jasper single-beam ultra violet and visible spectrophotometer at 660 nm **(Olsen et al., 1954)**. Available potassium (K) was analyzed by flame photometry using a Metzer Flame Photometer **(Toth and Prince, 1949)**.

The mean weighted value for every evaluated soil characteristic (V) was calculated by multiplying the parameter value (Vi) of each horizon by its thickness (ti) and then dividing the sum by the total depth of the soil profile (T). This calculation was performed using the following equation:

$$V = \sum_{n=1}^{\infty} \frac{(Vi \times ti)}{T}$$

2.3 Climatic Conditions

Aswan's climate (2014-2023) is characterized by extreme seasonal variations. Temperature patterns show hot, dry summers (May-Oct) with a peak average maximum temperature of 37.94°C in August and cool, dry winters (Dec-Mar) with a minimum average minimum temperature of 7.13°C in January. The significant temperature range classifies the soil as "thermic" (temperature) and "torric" (moisture). Rainfall is minimal, peaking at 7.82 mm in March, with a prolonged dry season (Jun-Oct). Relative humidity fluctuates, reaching its lowest at 29.91% in May and highest at 61.42% in December. Wind speed ranges from 8.22 km/h in January to 12.98 km/h in September.

2.4. Statistics analyses

Descriptive statistical data (range, minimum, maximum, mean, standard deviation, coefficient of variation (CV), skewness, and kurtosis) were calculated using SPSS 17 to describe soil variability. **Wilding (1985)** defined low variability as CV < 15%, moderate as 15%-35%, and high as CV > 35%.

In ArcGIS 10.8.3., the researched soil data were connected to the sampling location (spatial). Programs and maps showing the spatial distribution were prepared to determine the diversity of recognized soil properties. With the use of point data, ArcMap GIS 10.2.2 generated maps of a variety of soil parameters, including EC_e, pH, O.M, CEC, $CaCO_3$, ESP, SAR_e, (N), (P), (K), and texture. The addition for geostatistical analysis in ArcGIS 10.8.3 was used to conduct geostatistical analysis **(ESRI, 2019)**.

The Kriging procedure utilizes a semivariogram model, a mathematical function that describes spatial relationships, fitted to the data using weighted missing squares, range, nugget, and sill. Among Kriging methods, Ordinary Kriging (OK) is favored for its clarity and accuracy **(Isaaks**

and Srivastava 1989). However, Kriging methods, including OK, are most effective when the data is approximately normally distributed **(Johnston et al., 2001)**. The Kriging procedure is calculated using equation (1) (Webster and Oliver, 2007).

$$Z^* (X_0) = \sum_{i=1}^{N} \lambda i \, Z(X_i) \qquad\qquad (1)$$

Here, n is the number of locations used for interpolation, $Z(X_0)$ is the predicted value at an unsampled site X_0, $Z(X_i)$ is the measured value at location X_i, and λi is the weight assigned to $Z(X_i)$. Data points x_i are selected within a specified nearness.

To ensure whether the data were normally distributed and exhibited equal variance, data transformations were applied. Histograms and normal QQ plots were utilized to identify the necessary data adjustments for achieving a more normal distribution. Transformation techniques were used to verify the normal distribution of each soil characteristic.

Of these trends, logarithmic transformations were used to normalize outliers and highly skewed data sets **(Webster and Oliver, 2007)**. The main technique used to examine the spatial distribution of soil attribute structure is semi-variograms. According to **Wang and Shao (2013),** they were calculated using Equation (2), which is predicated according to the localized approach of variables and intrinsic assumptions **(Nielsen and Wendroth, 2003).**

$$\gamma(h) = \frac{1}{2N(h)} \sum_{i=1}^{N(h)} [Z(X_i) - (X_i + h)^2] \qquad\qquad (2)$$

n(h) represents the number of sample pairs within the lag interval distance h, whereas the real semi-variogram score at that distance is shown by $\gamma(h)$. $Z(X_i)$ and $Z(X_i + h)$ represent the sample values at the two spatial locations X_i and $X_i + h$, respectively.

Several semi-variogram models, including Stable, J-Bessel, K-Bessel, Hole Effect, Rational Quadratic, Gaussian, Exponential, Pentaspherical, Tetraspherical, Spherical, and Circular, were evaluated using cross-validation to ascertain which model best suited each soil feature. Error metrics such as Mean Error (ME), Mean Standard Error (MSE), Root Mean Square Error (RMSE), Average Standard Error (ASE), and Root Mean Square Standardized Error (RMSSE) were used to evaluate the predictive ability of these models. These metrics were calculated using equations (3) to (7), respectively. More accurate forecasts are shown by lower values of these error measures.

$$ME = \frac{1}{N} \sum_{i=1}^{N} [Z^*(X_i) - Z(X_i)] \qquad\qquad (3)$$

$$MSE = \frac{1}{N} \sum_{i=1}^{N} \left[\frac{Z^*(X_i) - Z(X_i)}{\delta^2(X_i)} \right] \qquad\qquad (4)$$

$$RMSE = \sqrt{\frac{1}{N} \sum_{i=1}^{N} [Z^*(X_i) - Z(X_i)]} \qquad\qquad (5)$$

$$\text{ASE} = \sqrt{\frac{1}{N} \sum_{i=1}^{N} \delta^2(X_i)} \qquad\qquad (6)$$

$$\text{RMSSE} = \sqrt{\frac{1}{N} \sum_{i=1}^{N} \frac{Z^*(X_i) - Z(X_i)}{\delta^2(X_i)}} \qquad\qquad (7)$$

The premise of equal variance in the data was satisfied and the data was made normally distributed by the application of transformations. Modifications to normalize the data were identified using QQPlots and histograms in ArcGIS statistical analysis. Every soil characteristic was subjected to a trend analysis. When dealing with severely skewed and anomalous data, logarithmic transformations were employed. In this research, the semivariogram models were tested for each property data set. Prediction performance was evaluated by cross-validation that checks The precision of the produced surfaces. Cross-validation helps us to identify which model delivers the best predictions. According to **Johnston et al. (2001)**, a model must have mean standardized error (MSE) values near zero, average standard error (ASE) values as minimal as feasible (helpful for comparing models), and root mean square standardized error (RMSSE) values near one in order to produce reliable predictions.

3. Results and discussion

3.1. Descriptive statistics

The soil properties displayed considerable variability across the investigated soil profiles as shown in the table (1). Significant differences were observed among the profiles in terms of mean, minimum, maximum, range, standard deviation, coefficient of variation, skewness, and kurtosis values. Some properties, such as available nitrogen, available potassium, and exchangeable sodium percentage (ESP), exhibited substantial disparities between their minimum and maximum values, whereas pH and organic matter (OM) had relatively smaller ranges.

The mean values ranged from 2.85 to 449.58, with high values observed for available potassium, sand, available nitrogen, and CEC, and low values for other properties. The standard deviation varied from 0.50 to 278.53, indicating that some properties, like pH and OM, had values clustered around the mean, while others, such as available nitrogen, available potassium, and ESP, were more dispersed.

The coefficient of variation (CV) ranged from 2.05% to 32.80%, with pH showing the lowest variability and the rest of the properties exhibiting moderate to high variability. This variability can be attributed to factors like agricultural management practices, soil type, and climate conditions. Salinity, being highly susceptible to these factors, showed the highest variability, while pH, due to soil buffering capacity, showed the lowest.

Most soil properties, except pH, OM, and sand, exhibited positive skewness, indicating non-normal distribution. Logarithmic transformation was applied to normalize these skewed datasets. Kurtosis values also indicated non-normality for most properties, necessitating transformation prior to geostatistical analysis.

Table 1: Descriptive statistics of the studied soil properties.

Property	Range	Min.	Max.	Mean	St.D	CV%	Skewness	Kurtosis
CaCo$_3$ (%)	22.06	2.45	24.51	10.28	4.71	15.27	0.77	0.33
O.M (%)	4.31	1.00	5.31	2.85	1.26	14.70	0.14	-1.05
pH(1:1)	1.85	7.15	9.00	8.15	0.50	2.05	-0.21	-0.74
ESP (%)	65.44	0.75	66.19	16.59	15.67	31.50	1.62	2.06
Sand (%)	64.32	25.92	90.24	64.17	12.35	6.42	-0.72	0.85
silt (%)	57.28	4.08	61.36	19.49	9.24	15.80	1.52	4.67
Clay (%)	51.12	4.92	56.04	16.34	10.00	20.40	1.47	2.56
CEC"meq/100g"	39.70	9.82	49.51	22.53	12.84	18.99	0.81	-1.11
EC$_e$ dS/m	45.77	1.58	47.35	7.66	7.54	32.80	3.08	12.72
SAR$_e$	57.94	2.57	60.51	10.74	9.57	29.72	3.08	12.36
k (mg.kg^{-1})	1356.52	19.33	1375.85	449.58	278.53	20.65	0.49	0.19
N (mg.kg^{-1})	160.00	5.00	165.00	32.78	24.21	24.62	2.80	11.53
P (mg.kg^{-1})	18.02	2.98	21.00	8.60	3.98	15.43	1.30	1.52

CV= Coefficient of Variation, St.D = Standard Deviation

3.2. The relationships between the investigated soil characteristics.

Data in table (2) show the correlation coefficients among the studied soil properties of the soil profiles. There is a negative correlation (at P=0.01) between the sand fraction and each of CEC, K, clay and silt. Moreover, there is a notably favorable association (at P=0.01) between clay and each of CEC and k, as well as CaCO$_3$ and each of K and EC$_e$, also EC$_e$ and both of SAR$_e$, ESP and K, in addition to ESP and both of pH and SAR$_e$. The positive correlation between CaCo$_3$ and K may be due to the fact that calcium carbonates fix high amounts of K, making potassium less susceptible to leaching into the soil. The negative correlation between sand and each of silt and clay is because the sum of all fractions equals a unchanged value (100%), so the rise in any of them offset by the decrease in the rest.

The negative relationship between sand and potassium is due to the fact that the sand part does not have the ability to exchange cations because it does not carry electrical charges, which makes it lose ions such as potassium easily through leaching. However, the negative correlation between sand and CEC is due to the inability of sand to exchange cations due to its lack of electrical charges, causing a negative correlation with CEC **(Blume et al., 2016)**. The correlation between clay and CEC is high (r = 0.74), and it is due to, as it is known, that the clay has a great capacity to adsorb and hold cations because its particle surfaces are very rich in negatively-charged sites.

A positive correlation was obtained between EC$_e$ and both ESP and SAR. The soils of the study area in some parts contain elevated values of dissolvable salts predominated by sodium ions (Na$^+$) concluding in a significant positive correlation between EC$_e$ and ESP. The positive relationship between ESP and pH is due to the effect of ESP on increasing pH. A positive correlation was obtained between EC$_e$ and both K and CaCo3, which is due to the fact that increasing K and CaCo$_3$ in the soil increases EC$_e$. The results showed that the correlation between

soil parameters for nitrogen, phosphorus, and organic matter is low due to the wide spatial variation of these properties.

Table (2): Correlation coefficients of the analyzed soil properties.

	O.M	CaCo$_3$	pH	EC$_e$	SARe	ESP	CEC	Sand	silt	Clay	N	P	K
O.M	1												
CaCo$_3$	0.420*	1											
pH	0.089	0.115	1										
EC$_e$	0.405*	0.493**	0.343	1									
SAR$_e$	0.359	0.362	0.221	0.918**	1								
ESP	0.425*	0.394*	0.515**	0.829**	0.683**	1							
CEC	-0.088	0.280	-0.186	0.160	0.260	-0.271	1						
Sand	0.042	-0.196	-0.227	-0.337	-0.417	-0.019	-0.660**	1					
Silt	-0.154	-0.038	0.276	0.203	0.262	0.154	0.122	-0.682**	1				
Clay	0.114	0.304	-0.002	0.226	0.268	-0.145	0.749**	-0.583**	-0.197	1			
N	0.069	0.166	-0.301	0.312	0.438*	0.044	0.124	-0.080	-0.017	0.126	1		
P	0.356	0.221	0.259	0.188	0.160	0.447*	-0.301	0.111	-0.019	-0.127	0.042	1	
K	0.309	0.496**	0.307	0.504**	0.408*	0.371	0.262	-0.496**	0.208*	0.433**	0.080	0.100	1

*Correlation is significant at the 0.05 level (2-tailed).

** Correlation is significant at the 0.01 level (2-tailed).

3.3. Geostatistics and spatial analysis

To assess the normality of the soil property data (Table 3), histograms and normal Q-Q plots were employed. While some properties, including pH, organic matter (OM), potassium (K), sand, and silt, exhibited normal distributions, others required a log transformation to achieve normality. By analyzing maps that show how soil characteristics vary across an area and understanding how these characteristics affect plant growth, decision-makers can pinpoint regions with high, medium, and low soil quality **(Vasu et al., 2017).**

As illustrated in Figure 2, potassium (K), a normally distributed property, displays a One-dimensional form, a small positive skewness value (0.30) approaching 0, and a kurtosis value (2.15) close to 2.0, indicating a normal distribution. In contrast, EC$_e$, a skewed property, necessitated a log transformation to normalize its distribution. Analyzing spatial distribution maps of soil properties can aid in identifying regions with varying soil quality, informing decisions related to plant growth. Figures 3, 4, 5, and 6 depict the locative distribution of selected soil properties. Clay fraction and CEC exhibit similar spatial patterns due to their strong positive correlation. Similarly, ESP, EC$_e$, and SAR share congruent spatial distributions, with the exception of soil salinity.

The locative distribution of the sand fraction was inversely related to the clay fraction. No discernible spatial trends were observed for pH, nitrogen (N), phosphorus (P), OM, CaCO$_3$, and K.

The generated spatial distribution maps (Figures 3, 4, 5, and 6) categorize soil characteristics, identifying areas suitable for cultivation and those requiring careful management. These maps

provide valuable insights into the spatial variability of soil attributes within the study region, enabling the implementation of site-specific management practices.

Table 3: Weighted means of soil properties for the investigated profiles in the research area.

Profile No.	O.M (%)	CaCo₃ (%)	pH	ECₑ dS/m	SARₑ	Esp (%)	CEC (meq/100)	N	P	k	Particle size distribution			Soil texture
									(mg.kg⁻¹)		Sand %	Silt %	Clay %	
1	3.44	9.76	7.83	3.76	7.90	7.81	12.09	30.00	7.68	792.01	54	18	28	Sandy Clay loam
2	1.68	5.21	7.72	3.10	5.55	6.34	12.76	30.00	6.09	218.81	77	10	13	sandy loam
3	2.78	6.13	7.79	2.36	4.80	1.81	12.86	30.33	4.21	349.15	57	34	9	sandy loam
4	3.39	7.21	7.62	7.37	11.79	7.89	13.09	28.46	8.87	132.88	64	15	21	Sandy Clay loam
5	3.05	10.83	8.28	2.73	5.76	7.42	13.64	36.33	6.33	265.36	58	22	19	sandy loam
6	2.37	14.83	7.53	3.21	5.67	5.61	14.47	22.00	8.64	194.88	63	19	18	sandy loam
7	1.42	13.56	8.64	6.01	10.57	8.65	15.03	16.33	6.40	738.81	49	28	24	Sandy Clay loam
8	1.67	7.72	8.32	8.66	12.40	15.06	17.08	24.00	8.29	518.05	42	52	6	silt loam
9	2.31	9.93	8.02	5.96	8.18	18.73	17.93	39.00	13.77	422.29	65	21	14	sandy loam
10	1.73	8.62	8.43	9.82	10.42	9.80	17.97	25.67	7.65	609.81	38	19	43	Clay
11	1.46	6.29	8.41	6.26	9.07	19.26	19.79	27.00	6.17	282.65	67	21	12	sandy loam
12	2.08	7.51	8.33	6.84	10.97	12.31	20.51	30.00	10.79	443.24	53	29	19	sandy loam
13	2.08	14.09	7.62	2.80	4.17	3.42	20.57	40.33	8.53	343.83	77	12	12	sandy loam
14	1.63	3.39	8.26	2.27	3.29	8.61	20.59	33.08	9.33	57.69	80	10	10	sandy loam
15	1.87	4.08	8.17	2.44	3.25	10.93	22.03	25.00	6.27	339.84	68	19	13	sandy loam
16	2.49	12.25	8.15	2.89	5.90	17.67	22.21	25.00	13.15	310.58	70	15	14	sandy loam
17	3.55	11.27	8.70	10.94	16.86	35.19	26.44	24.00	11.68	174.93	61	28	11	sandy loam
18	3.14	9.68	7.70	6.40	10.58	9.21	27.88	25.67	6.39	311.91	64	13	22	Sandy Clay loam
19	3.71	11.23	8.40	16.49	20.85	56.56	31.32	19.33	12.12	619.12	70	22	8	sandy loam
20	2.93	22.21	8.47	19.27	16.91	43.21	31.51	31.25	7.08	557.94	65	20	15	sandy loam
21	3.42	13.93	8.11	24.66	43.42	35.33	33.36	58.33	8.74	643.06	46	25	29	Sandy Clay loam
22	2.12	4.76	7.95	3.81	5.48	5.46	33.51	28.08	5.91	266.38	82	8	10	loamy sand
23	3.93	10.05	8.52	3.74	4.91	14.73	33.95	21.67	10.62	293.29	70	15	15	sandy loam
24	3.60	17.92	8.23	12.72	15.40	19.54	33.96	22.50	7.86	632.75	59	9	32	Sandy Clay loam
25	3.76	12.05	8.44	2.64	3.64	10.31	34.44	22.00	10.43	605.82	69	13	17	sandy loam
26	3.95	18.38	8.16	13.17	13.21	28.35	38.87	41.92	11.19	884.80	62	18	19	sandy loam
27	3.61	6.66	8.53	14.85	15.89	39.46	41.30	21.33	9.57	592.52	69	20	11	sandy loam

K

EC_e before Log Transformation
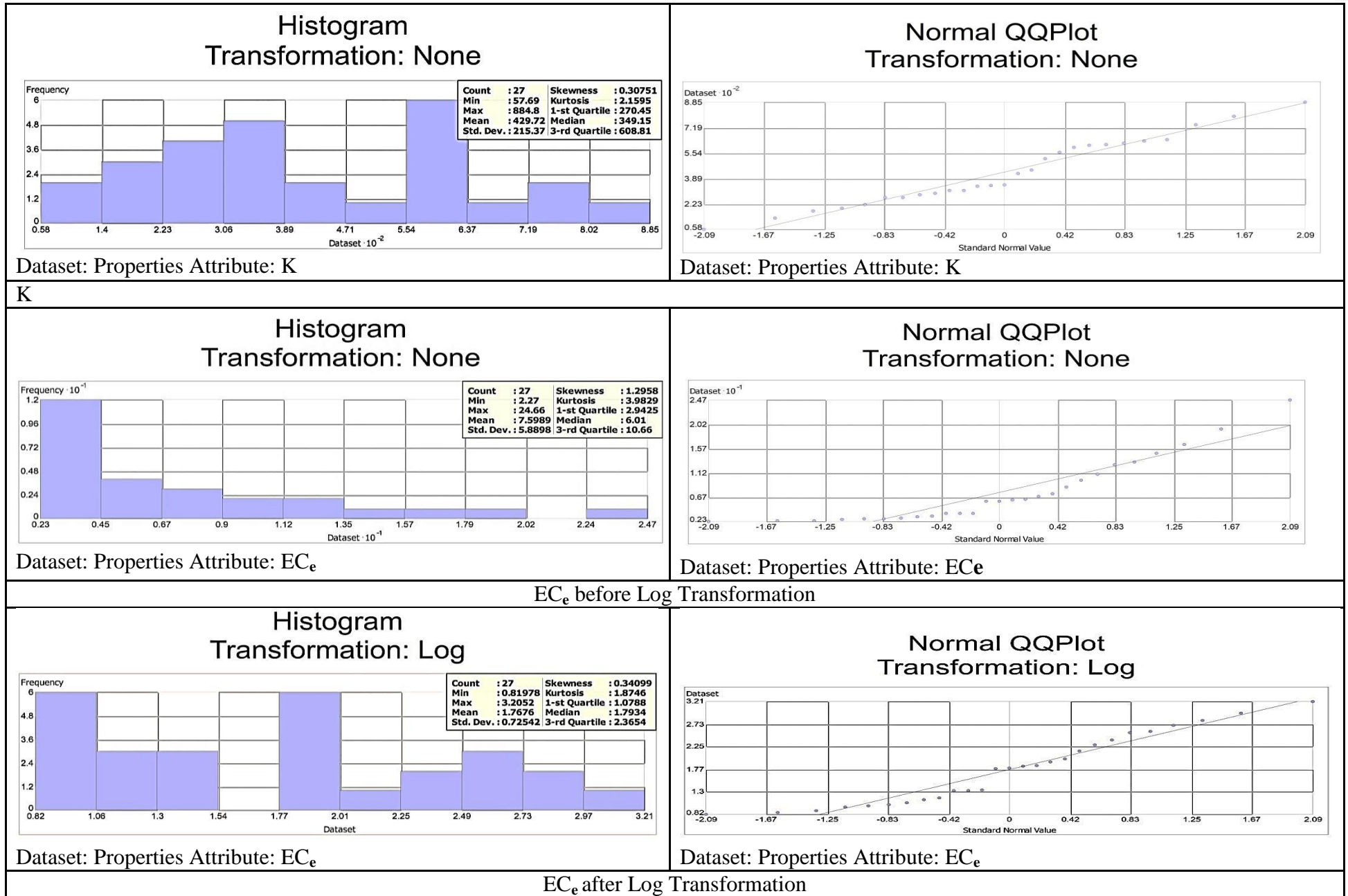
EC_e after Log Transformation

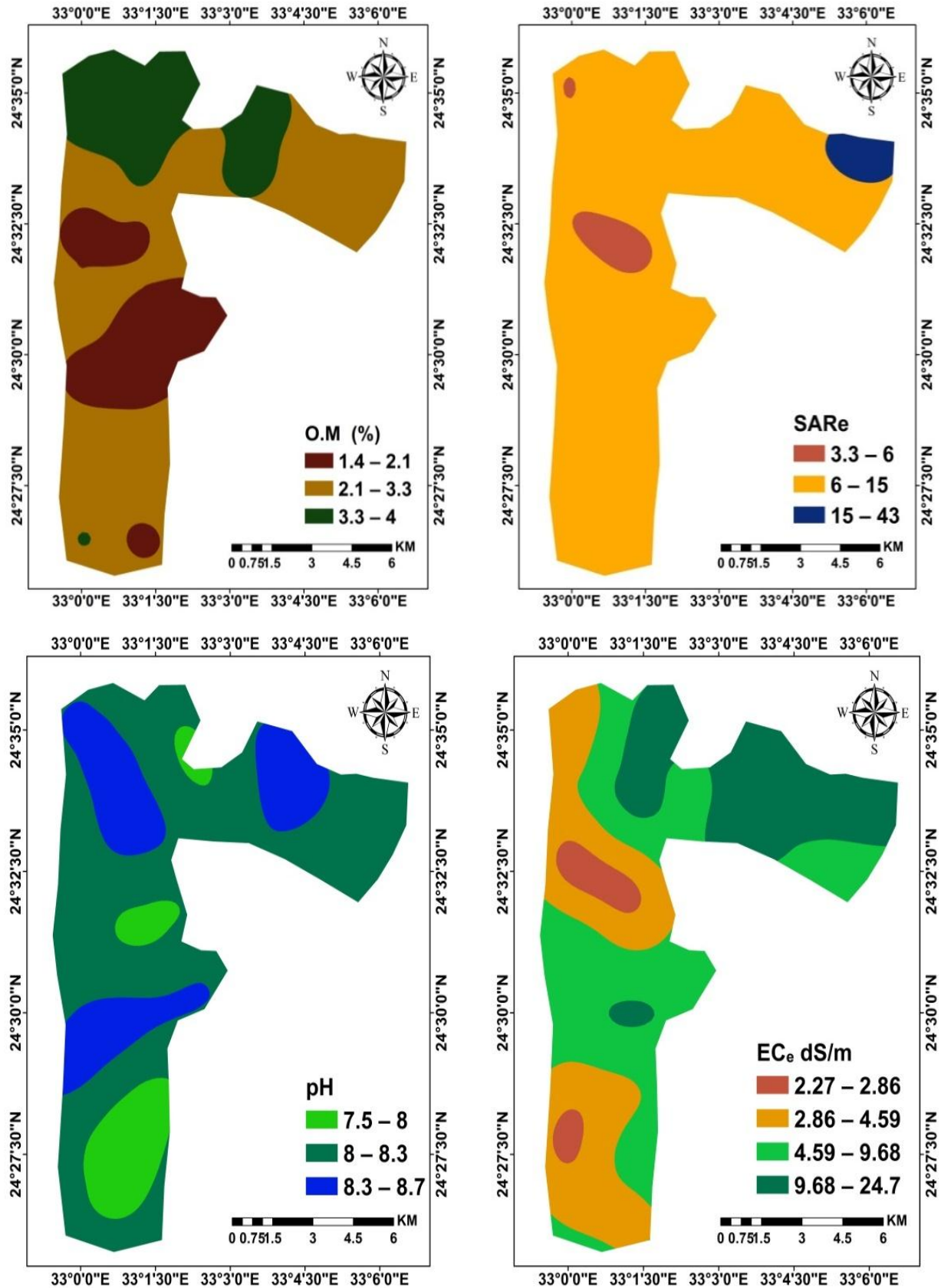**Figure (2): QQPlot with histograms for ECe (before and after log transformation) and K (normally distributed).**

Figure (3): Maps of spatial distribution for pH, EC$_e$, SAR$_e$ and O.M in the studied area.
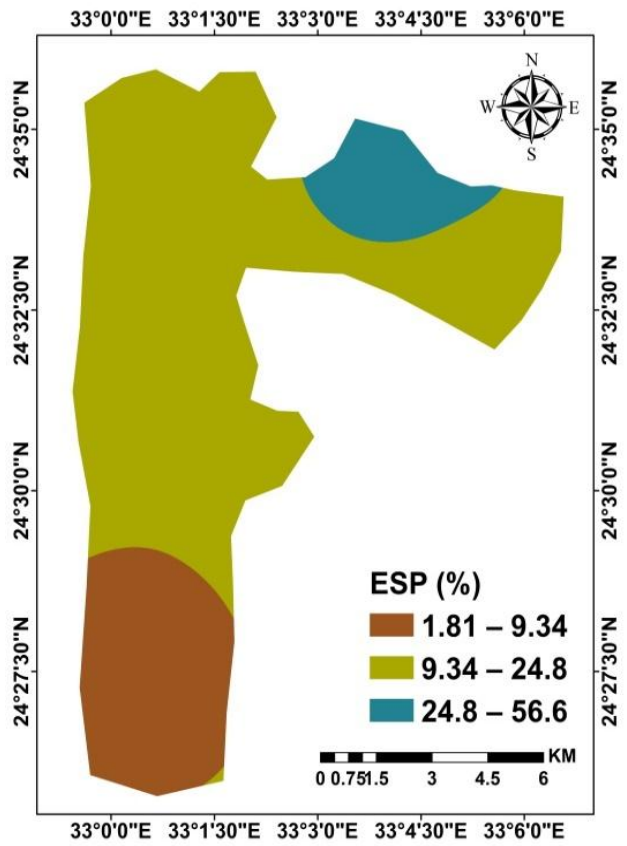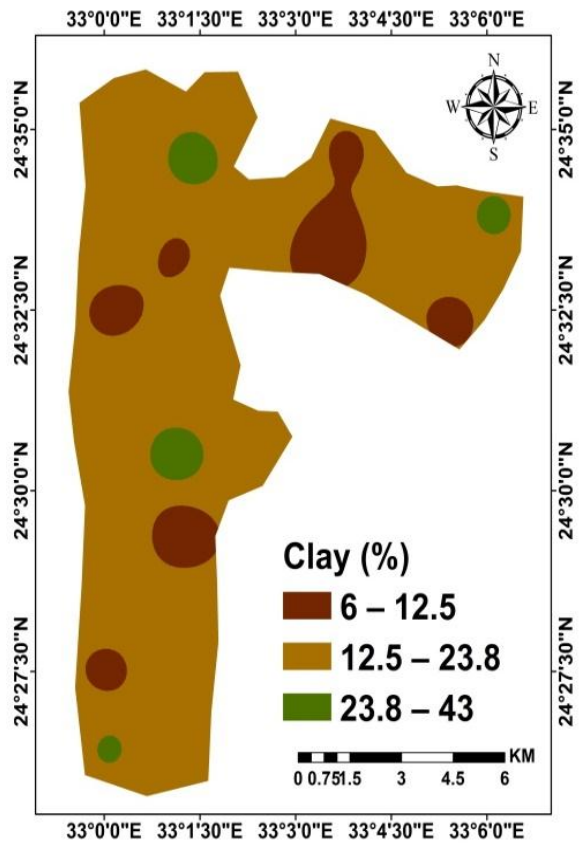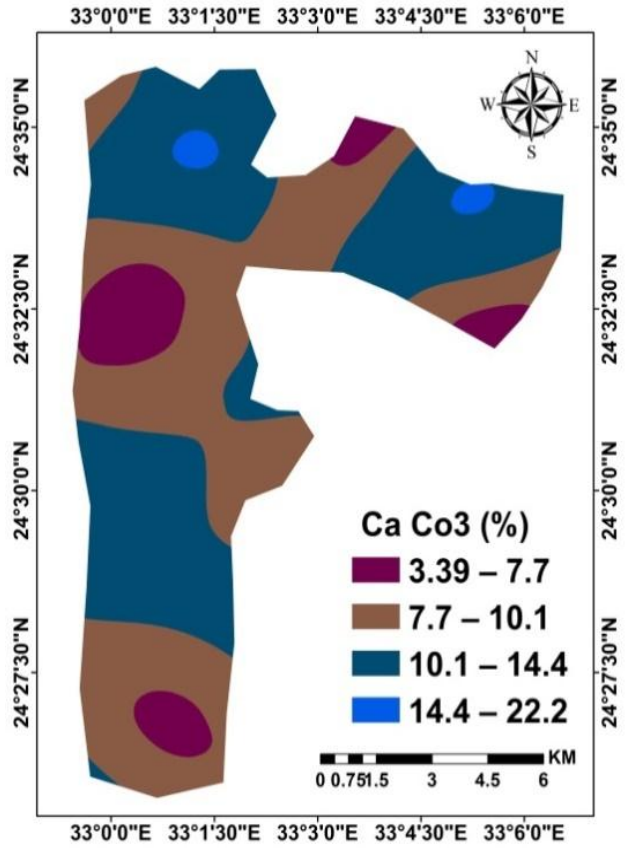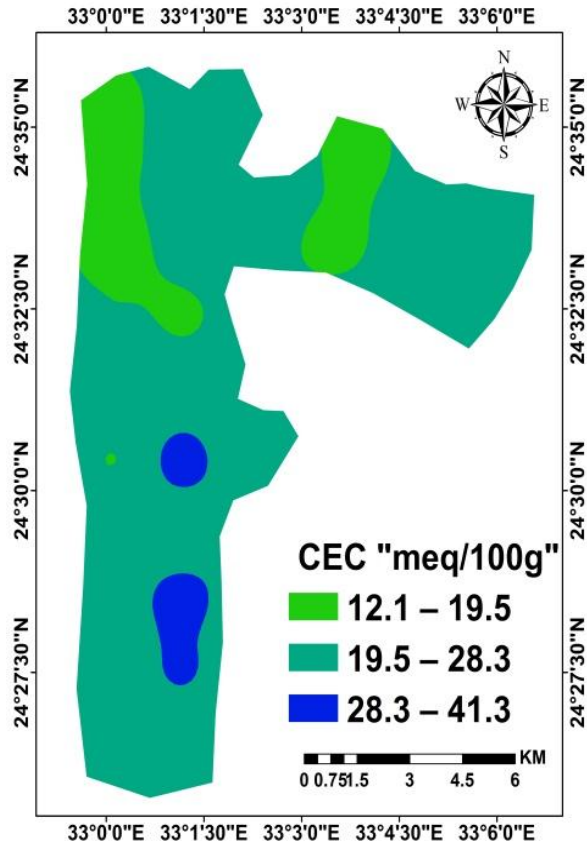
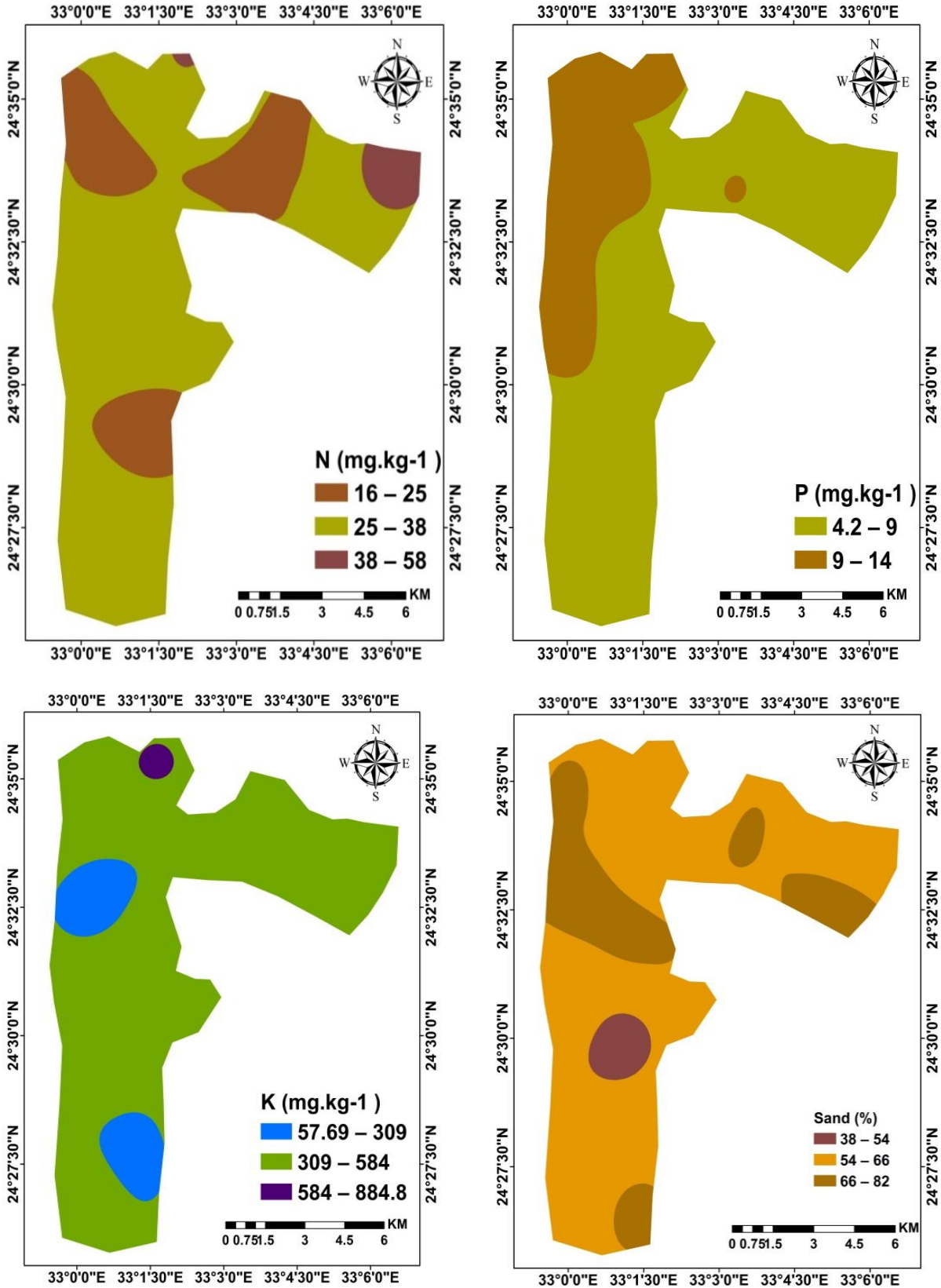**Figure (4): Maps of spatial distribution for ESP, CaCo₃ , CEC and Clay in the studied area.**

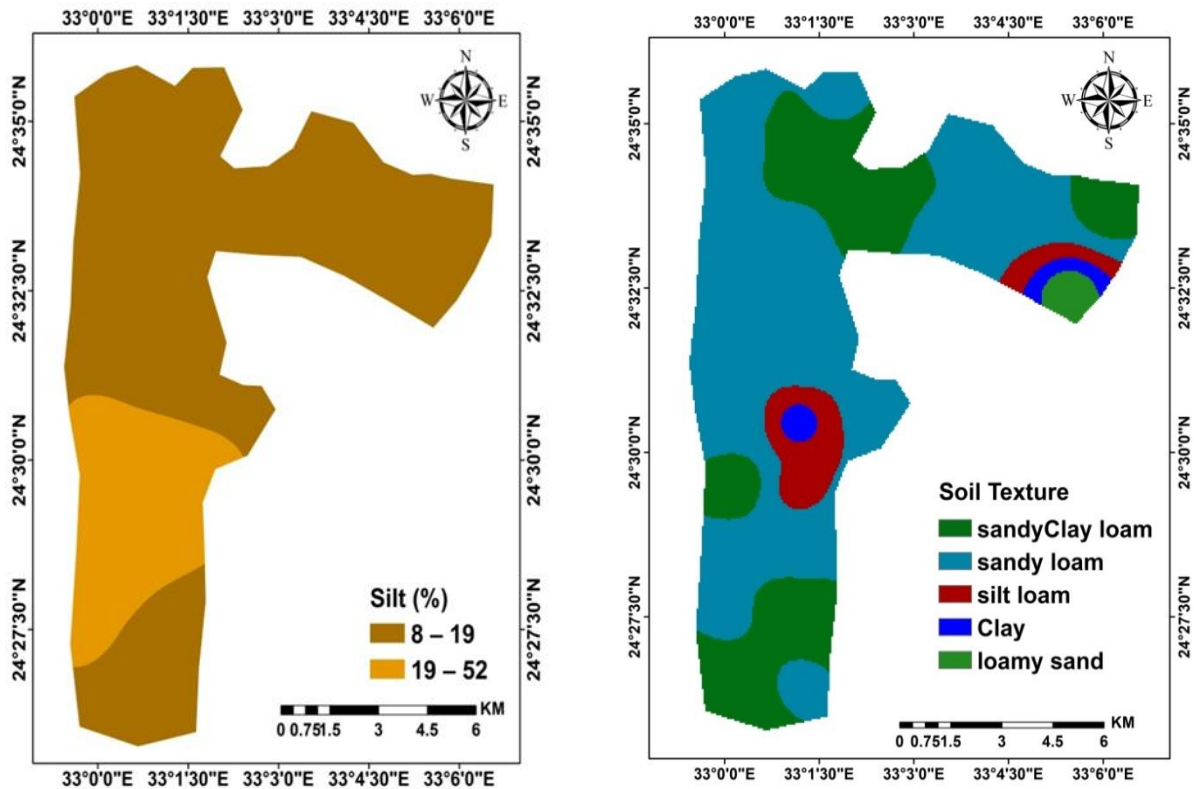**Figure (5): Maps of spatial distribution for N, P, K and Sand in the studied area.**

Figure (6): Maps of spatial distribution for Silt and Soil texture in the studied area.

In the present study, the semivariogram models (Exponential, Gaussian, K-Bessel and J-Bessel) are examined for each soil property data set. The cross validation evaluates prediction capabilities by looking at the generated surfaces' correctness. The cross-checking procedure technique is used to determine the best accurate predictions for soil properties with the lowest mean standardized error (MSE) values (around zero) after using different models for every soil attribute that was examined in this research. The smallest MSE values suggest kriging predictions of soil parameters that are closest to the observed values. The models that produce the best outcomes are selected.

Table 4: Semivariogram models for the soil properties of the studied profiles.

Properties	Models	Errors in Prediction						
		Mean	RMS	ASE	MS	RMSSE	Skewness	Kurtosis
CaCo$_3$ (%)	J-Bessel	-0.06	4.30	4.23	-0.02	1.02	-0.31	2.53
O.M (%)	Exponential	-0.02	0.65	0.74	-0.02	0.86	-0.05	1.51
pH	J-Bessel	0.00	0.30	0.31	-0.01	0.97	-0.38	2.02
ESP(%)	Gaussian	0.45	12.39	15.18	0.04	0.72	-0.12	2.80
Sand (%)	K-Bessel	-0.381	10.61	10.48	-0.03	1.01	-0.45	2.83
Silt (%)	Gaussian	0.01	8.92	8.62	0.00	1.02	0.14	3.05
Clay (%)	Exponential	-0.58	10.27	5.06	-0.42	2.41	1.31	4.65
CEC "meq/100g"	Gaussian	0.55	8.61	8.43	0.05	1.02	0.36	1.81
EC$_e$ dS/m	K-Bessel	-0.04	4.82	7.84	0.01	0.67	0.24	1.87
SAR$_e$	Gaussian	-0.54	7.61	6.66	-0.05	1.09	2.51	10.78

Properties	Models	Errors in Prediction						
		Mean	RMS	ASE	MS	RMSSE	Skewness	Kurtosis
k (mg.kg-1)	K-Bessel	-8.73	204.11	205.06	-0.03	0.99	0.30	2.15
N (mg.kg-1)	J-Bessel	0.14	7.81	6.81	0.02	1.12	1.57	6.12
P (mg.kg-1)	Exponential	0.03	2.34	2.34	0.01	1.00	0.37	2.37

The abbreviations are as follows: **RMS**: Root Mean Square, **ASE**: Average Standard Error, **MS**: Mean Standardized and **RMSSE**: Root Mean Square Standardized Error.

Table 4 presents the best-performing templates as well as their corresponding incorrect prediction values for each examined soil attribute. The table also highlights that alternative models may yield superior results for specific soil properties. While the mean standardized error (MS) values are close to zero, the root mean square standardized error (RMSSE) values range from 0.67 to 2.41 (approaching two). These findings demonstrate that the selected semivariogram models effectively represent the spatial variability of the soil attributes, making them ideal for generating accurate spatial distribution maps.

4. Conclusions

The results showed that the soils in the study area exhibited a little to middling alkaline and a little to highly saline conditions, with varying levels of sodicity. The particle size distribution was highly variable, resulting in a wide range of soil textures, from sandy to clay. Organic matter content was moderate, and capacity for cation exchange varied from low to high. Log-transformation proved effective in normalizing skewed datasets. Semivariogram models were found to be suitable for all investigated soil properties. Double-checking was utilized to identify the best-fitting model for each property. Gaussian, J-Bessel, Exponential, and K-Bessel models emerged as the most appropriate for different soil properties. The generated maps categorize soil characteristics, identifying areas suitable for cultivation and those requiring careful management. These maps help understand how soil properties influence plant growth and identify regions with high, medium, and low soil quality, aiming to increase soil productivity and mitigate limitations.

5. Acknowledgment

6. References

AbdelRahman, M. A. E., Shalaby, A. and Belal, A. A. (2017). A GIS Based Model for Land Evaluation Mapping: A Case Study North Delta Egypt. Egyptian Journal of Soil Science, 57(3), 339-351.

AbdelRahman, M.A.E., Zakarya, Y.M., Metwaly, M.M. and Koubouris, G.D. (2021). Deciphering soil spatial variability through geostatistics and interpolation techniques. Sustainability 13, 194. https://doi.org/10.3390/su13010194.

Abdullahi, M. B., Elnaggar, A. A., Omar, M. M., Murtala, A., Lawal, M. and Mosa, A. A. (2023). Land degradation, causes, implications and sustainable management in arid and semi arid regions: a case study of Egypt. Egyptian Journal of Soil Science, 63(4), 659-676.

Arnous, M. O. and Hassan, M. A. A. (2006). Image processing and land information system for soil assessment of El-Maghara Area, North Sinai, Egypt. In International Conf. on Water Resources and Arid Environment.

Blume, H. P., Brümmer, G. W., Fleige, H., Horn, R., Kandeler, E., Kögel-Knabner, I. and Wilke, B. M. (2016). Chemical properties and processes. Scheffer/SchachtschabelSoil Science, 123-174.

Bogunovic, I., Pereira, P. and Brevik, E. C. (2017). Spatial distribution of soil chemical properties in an organic farm in Croatia. Science of the total environment, 584, 535-545.

Brevik, E. C., Calzolari, C., Miller, B. A., Pereira, P., Kabala, C., Baumgarten, A. and Jordán, A. (2016). Soil mapping, classification, and pedologic modeling: History and future directions. Geoderma, 264, 256-274.

Cruz, J. S., de Assis Júnior, R. N., Matias, S. and Tamayo, J. H. C. (2011). Spatial variability of an Alfisol cultivated with sugarcane. Ciencia e investigación agraria: revista latinoamericana de ciencias de la agricultura, 38(1), 155-164.

ESRI (2019). Are Map version 10.2.2. User Manual. ESRI, 380 New York Street Redlands, California, 92373- 8100, USA.

Everest, T. and Gür, E. (2022). A GIS-based land evaluation model for peach cultivation by using AHP: a case study in NW Turkey. Environmental Monitoring and Assessment, 194(4), 241.

Fathi H., H. Fathi and H. Moradi (2014). Spatial variability of soil characteristics for evaluation of agricultural po tential in Iran Merit Research. J. of Agric. Sci. and Soil Sci., 2(2):024-031. DOI:10.3923/jest.2015.13.24.

Ferreiro, J.P., Pereira De Almeida, V., Cristina Alves, M., Aparecida De Abreu, C., Vieira, S.R. and Vidal Vázquez, E., (2016). Spatial variability of soil organic matter and cation exchange capacity in an Oxisol under different land uses. Commun. Soil. Sci. Plant Anal. 47 (sup1), 75–89. https://doi.org/10.1080/ 00103624.2016.1232099.

Fraisse, C. W., Sudduth, K. A., Kitchen, N. R. and Fridgen, J. J. (1999). Use of unsupervised clustering algorithms for delineating within-field management zones.

Ghartey, E. O., Dowuona, G. N., Nartey, E. K., Adjadeh, T. A., Lawson, I. Y. (2012). Assessment of variability in the quality of an acrisol under different land use systems in Ghana. Open Journal of Soil Science, 2(1), 33-43.

Goenster-Jordan, S., Jannoura, R., Jordan, G., Buerkert, A. and Joergensen, R. G. (2018). Spatial variability of soil properties in the floodplain of a river oasis in the Mongolian Altay Mountains. Geoderma, 330, 99-106.

Goenster-Jordan, S., Jannoura, R., Jordan, G., Buerkert, A. and Joergensen, R. G. (2018). Spatial variability of soil properties in the floodplain of a river oasis in the Mongolian Altay Mountains. Geoderma, 330, 99-106.

Isaaks, E.H. and Srivastava, R.M., (1989). An introduction to applied geostatistics.Oxford. University Press, New York.

Issawi, B., Sallam, E. and Zaki, S. R. (2016). Lithostratigraphic and sedimentary evolution of the Kom Ombo (Garara) sub-basin, southern Egypt. Arabian Journal of Geosciences, 9, 1-17.

Jabro, J. D., Stevens, W. B., Evans, R. G. and Iversen, W. M. (2010). Spatial variability and correlation of selected soil properties in the Ap horizon of a CRP grassland. Applied Engineering in Agriculture, 26(3), 419-428.

Jackson, M. (1958). Soil chemical analysis prentice Hall. Inc., Englewood Cliffs, NJ, 498(1958), 183-204.

John, K., Abraham, I. I., Kebonye, N. M., Agyeman, P. C., Ayito, E. O. and Kudjo, A. S. (2021). Soil organic carbon prediction with terrain derivatives using geostatistics and sequential Gaussian simulation. Journal of the Saudi Society of Agricultural Sciences, 20(6), 379-389.

Johnston, K., Ver Hoef, J. M., Krivoruchko, K. and Lucas, N. (2001). Using ArcGIS geostatistical analyst (Vol. 380). Redlands: Esri.

Lima, T.M., Weindorf, D.C., Curi, N., Guilherme, L.R., Lana, R.M. and Ribeiro, B.T (2019). Elemental analysis of Cerrado agricultural soils via portable X-ray fluorescence spectrometry: inferences for soil fertility assessment. Geoderma 353, 264–272.https://doi.org/10.1016/j.geoderma.2019.06.045.

Liu, J., Yang, H., Zhao, M. and Zhang, X.H., (2014). Spatial distribution patterns of benthic microbial communities along the Pearl Estuary. China. Syst. Appl. Microbiol. 37 (8), 578–589. https://doi.org/10.1016/j.syapm.2014.10.005.

Nada, W. M., Bahnassy, M. H. and Ahmed, D. M. (2022). Soil maps based on GIS and ALES‐Arid Model as tools for assessing land capability and suitability in el-Sadat region of Egypt. Egyptian Journal of Soil Science, 62(4), 311-324.

Nielsen, D.R. and Wendroth, O., (2003). Spatial and temporal statistics-sampling field soils and their vegetation. Geoecology Textbook. Catena Verlag, Reiskirchen, Germany. https://doi.org/10.2136/vzj2005.0004br

Okashaa, E. G. M. (2023). Land Capability and Suitability Assessment of New Aswan Area, Aswan Governorate, Egypt. M.Sc. Thesis, Fac. of Agric. and Nat. Res. Aswan Univ., Aswan, Egypt.

Olsen, S. R. (1954). Estimation of available phosphorus in soils by extraction with sodium bicarbonate (No. 939). US Department of Agriculture.

Ouallali, A., Kader, S., Bammou, Y., Aqnouy, M., Courba, S., Beroho, M. and Hysa, A., (2024). Assessment of the Erosion and outflow intensity in the Rif region under different land use and land cover scenarios. Land 13 (2). https://doi.org/10.3390/ land13020141.

Richards, L. A. (1954). Diagnosis and improvement of saline and alkali soils. US Salinity Laboratory Staff, US Department of . Agriculture:Washington, DC, USA.

Rosemary, F., Vitharana, U.W.A., Indraratne, S.P., Weerasooriya, R. and Mishra, U., (2017). Exploring the spatial variability of soil properties in an Alfisol soil catena. Catena 150, 53–61. https://doi.org/10.1016/j.catena.2016.10.017.

Serrano, J., Shahidian, S. and Silva, J. M. D. (2014). Spatial and temporal patterns of apparent electrical conductivity: DUALEM vs. Veris sensors for monitoring soil properties. Sensors, 14(6), 10024-10041.

Soil Survey Laboratory, (1992). Procedures for collecting soil samples and methods of analysis for soil survey. Soil Survey Investigations Reports U.S. Govermentan Print Office, Washington D.C., USA.

Soil Survey Staff (2022). Keys to soil taxonomy.13th ed. United States Department of Agriculture, Natural Resources Conservation Service, Washington, DC.USA.

Subbiah, B. V. and, Asija, G. L. (1956). A rapid procedure for the estimation of available nitrogen in soils.

Tang, X.L., Xia, M.P., Pérez-Cruzado, C., Guan, F.Y. and Fan, S.H., (2017). Spatial distribution of soil organic carbon stock in Moso bamboo forests in subtropical China. Sci. Rep. 7, 1–13. https://doi.org/10.1038/srep42640.

Toth, S. J. and Prince, A. L. (1949). Estimation of cation-exchange capacity and exchangeable Ca, K, and Na contents of soils by flame photometer techniques. Soil science, 67(6), 439-446.

Tripathi, R., Nayak, A.K., Shahid, M., Raja, R., Panda, B.B., Mohanty, S., Kumar, A., Lal, B., Gautam, P. and Sahoo, R.N., (2015). Characterizing spatial variability of soil properties in salt affected coastal India using geostatistics and kriging. Arab J. Geosci. 8 (12), 10693–10703. https://doi.org/10.1007/s12517-015-2003-4.

Vasu, D., Singh, S.K., Sahu, N., Tiwary, P., Chandran, P., Duraisami, V.P., Ramamurthy, V., Lalitha, M. and Kalaiselvi, B., (2017). Assessment of spatial variability of soil properties using geospatial techniques for farm level nutrient management. Soil Tillage Res. 169, 25–34. https://doi.org/10.1016/j.still.2017.01.006.

Webster, R.. and Oliver, M.A., (2007). Geostatistics for environmental scientists, second ed. Chichester, United Kingdom, John Wiley & Sons pp.271. https:// onlinelibrary.wiley.com/doi/book/10.1002/9780470517277

Wilding, L.P. (1985). Spatial variability: its documentation, accommodation, and implication to soil surveys. P.166-194, in D.R. Nielsen and J. Bouma (ed.). Soil Spatial Variability, Pudoe, Wageningen,Netherlands.http://pascalfrancis.inist.fr/vibad/index.php?action=getRecordDetail&idt =8485840.

Zhang, H., Zhuang, S., Qian, H., Wang, F. and Ji, H. (2015). Spatial variability of the topsoil organic carbon in the Moso bamboo forests of southern China in association with soil properties. PloS one, 10(3), e0119175.